A multifunction trade-off has contrasting effects on the evolution of form and function

Katherine A. Corn, Christopher M. Martinez, Edward D. Burress, & Peter C. Wainwright

SUPPLEMENTARY INFORMATION

Methods

Dataset construction.—Fishes were classified as "suction feeders" if their primary mode of prey capture uses suction. We classified a "biting" feeding mode as one where the fish uses suction as well as direct biting actions. A direct biting action was designated as one where the fish's closing jaws make contact with the prey item to either grip it or scrape it from a holdfast. The number of strikes in our analyses for each species ranged from 2-9, with a median of 3. The number of individuals filmed for each species ranged from 1-3, with a median of 1 individual per species. All fishes were filmed feeding on minimally- or non-evasive prey and care was taken to induce high-effort strikes, where the fishes achieved a fully opened mouth. Protocols for animal care and experiments were approved by the University of California, Davis Institutional Animal Care and Use Committee (protocol #20475).

Landmark data.—Landmarks were chosen to capture the highest proportion possible of the motion of the fish's head during suction feeding strikes. Sliding semi-landmarks were designed to track changes in curvature along the ventral margin of the fish's head. Semi-landmarks were necessary in order to capture shape change along a structure with few features that could be identified to discrete, fixed points. In this case, they captured the curvature of the hyoid of the fish with eight equidistant semi-landmarks that were bounded on either end by fixed points at the insertion of the pelvic fin and at the base of the rostral tip of the dentary (Fig. S1). We measured kinematic components as the maximum value of each trait throughout the strike, regardless of whether that value occurred at peak gape. Measurements are depicted in Fig. S2.

Evolutionary model simulations.—To test the ability of our tree topology and character distribution to distinguish between different Brownian Motion or Ornstein-Uhlenbeck evolutionary models, we ran simulations in the R package *OUwie* (Beaulieu et al. 2012). We simulated data using our tree and discrete trait topology under each model that we fit in our analysis (single-rate Brownian Motion, BM1; multi-rate Brownian Motion, BMS; single-rate, single-optimum Ornstein-Uhlenbeck, OU1; single-rate, multi-optimum Ornstein-Uhlenbeck, OUM; multi-rate, multi-optimum Ornstein-Uhlenbeck, OUMV). First, we generated a distribution of 100 stochastic character maps of the discrete trait history using *phytools* (Revell 2012). Then, we simulated a dataset under each of the 5 models on each discrete trait history. We compared the fit of all 5 BM and OU models on each of the simulated datasets to see whether we could recover the model under which the traits had been simulated as the best-fit model.

Bayesian evolutionary model prior robustness.—To measure the effect of the prior we specified on the number of rate shifts, we ran alternative models with priors of 1, 5, and 10 rate shifts and compared its effect on posterior estimates of key parameters. The 1 and 10 shift prior models on the linear distance dataset MCMCs ran for 750,000 generations and the 5 shift prior model MCMC ran for 500,000 generations. The angles dataset MCMCs ran for 1 million generations. The overall kinesis dataset ran for 2 million generations and we ran an additional MCMC for the 10 shift prior for 3 million generations (see Results). All models ran with a with a 10% burn-in.

Results

Evolutionary model simulations.—Simulations suggested that we had moderately high ability to distinguish between evolutionary models, which may explain the similar fits of the OUMV model with either BMS or OUM models with our observed dataset. Most models that we fit were well- or moderately- able to be distinguished from other models, or were selected as the best model with one or more other models having comparable fits. 88% of the time, simulations run under BM1 were best-fit by BM1 alone or BM1 fit similarly as 1 or more other models. The other proportions of the time in which the simulated model was recovered as the best-fit were as follows: 44% BMS, 98% OU1, 92% OUM, and 78% OUMV.

Bayesian evolutionary model prior robustness.—We found that the estimated parameters were largely consistent across the three priors on the number of rate shifts in the angles and distances dataset (Figure S5). As expected, the posterior number of rate shifts in the continuous characters increased with the prior, but the posterior number of states changes and the rate ratio between the states were consistent across different priors. However, in the overall cranial kinesis data, we found some variation in the rate ratios between the states based on the prior on the number of rate shifts. It appears that the 1-shift prior model found a peak in parameter space where the rates of evolution between groups are different, but with higher rates of evolution in biters. It is likely that the 1-shift prior model has gotten stuck in an area of low likelihood, but with just one predicted shift, has few opportunities to traverse parameter space in search of another likelihood region. The 10-shift prior produced contrasting results across different runs, with a model run for 2 million generations mirroring the 1-shift results and a model run for 3 million generations mirroring the 5-shift results, indicating that there may be a local likelihood peak where the models support a faster rate in biters. However, with more generations of the MCMC, the model found a peak with suction feeders faster. This pattern may reflect issues outlined in Moore et al. (2016) where the prior on the number of rate shifts may constrain or overly influence the posterior, or highlight the benefit of running the MCMCs for additional generations.

SUPPLEMENTAL FIGURES

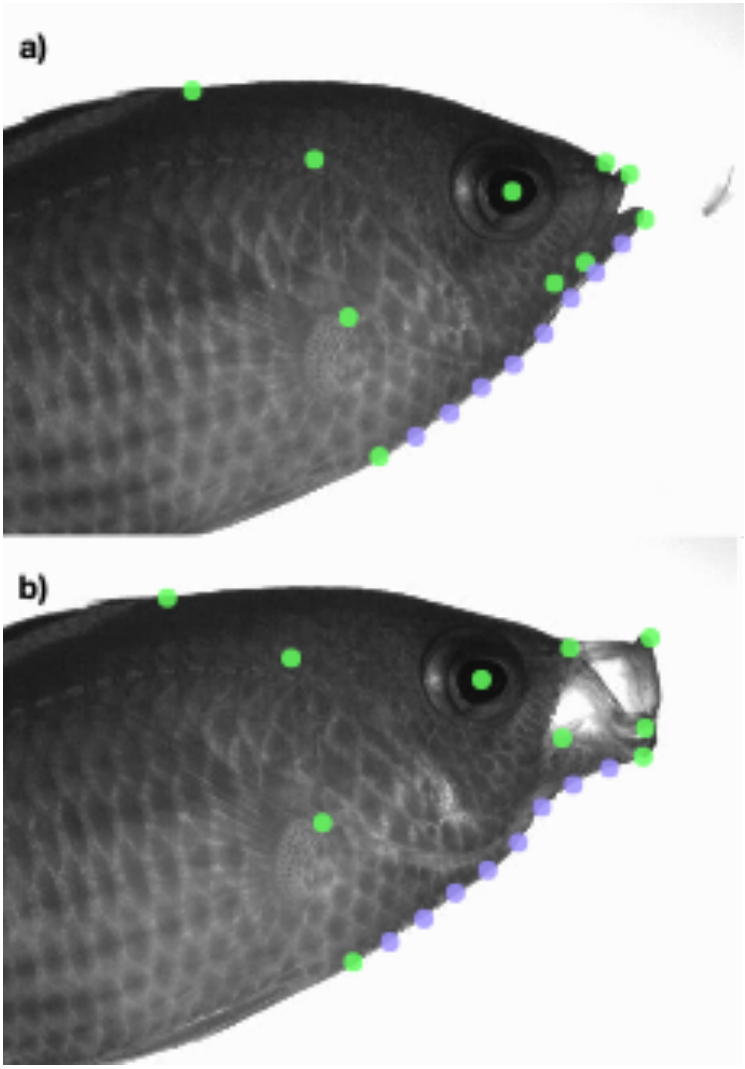

Fig. S1. —Landmarks on a fish at a) strike initiation and b) maximum gape. Ten green points indicate fixed landmarks. Purple points indicate the eight sliding semi-landmarks.

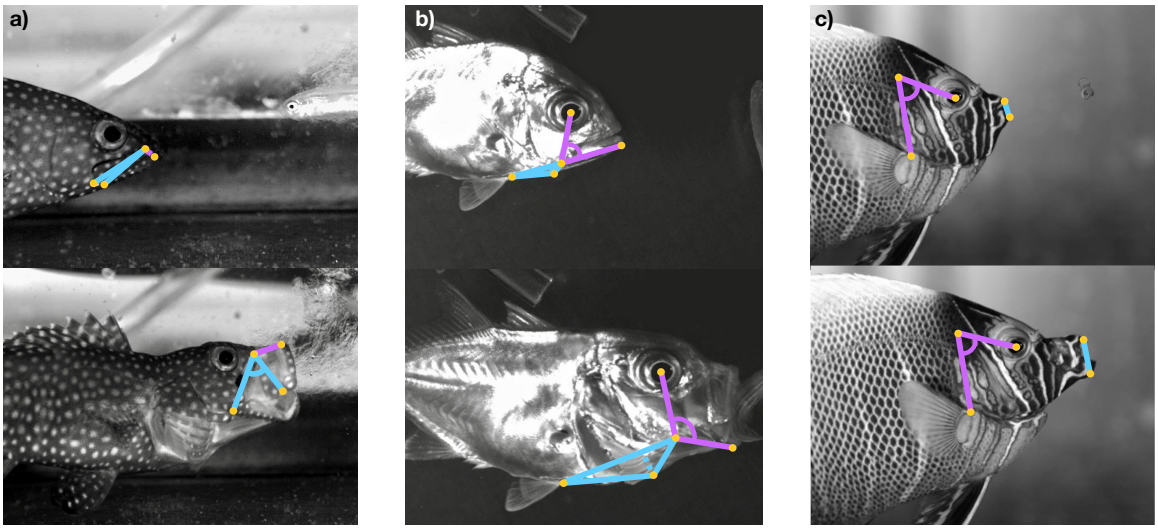

Fig. S2.—Angles and distances used to measure kinematic components. a) Blue indicates angle of maxillary rotation; purple displays premaxillary protrusion. b) Blue shows measurement of hyoid depression, as height of triangle; purple is angle of lower jaw depression. c) Blue indicates gape measurement; purple depicts angle of cranial elevation.

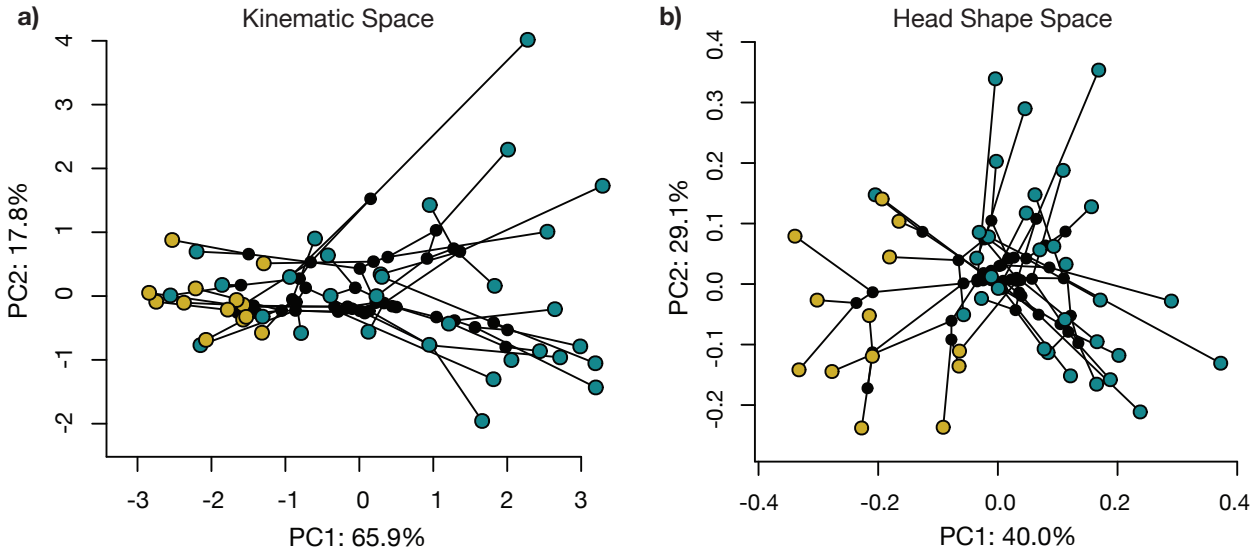

Fig. S3.—Plots of principle component axes 1 and 2 with lines displaying phylogenetic relationships between observations, species (depicted without phylogeny in Fig. 3). a), kinematic space occupation. b), cranial shape morphospace occupation. Notably, the kinematic PCA shows a relatively moderate effect of phylogenetic signal. In contrast, the head shape PCA shows a substantial effect of relatedness in the biting group and weaker effect in suction feeders.

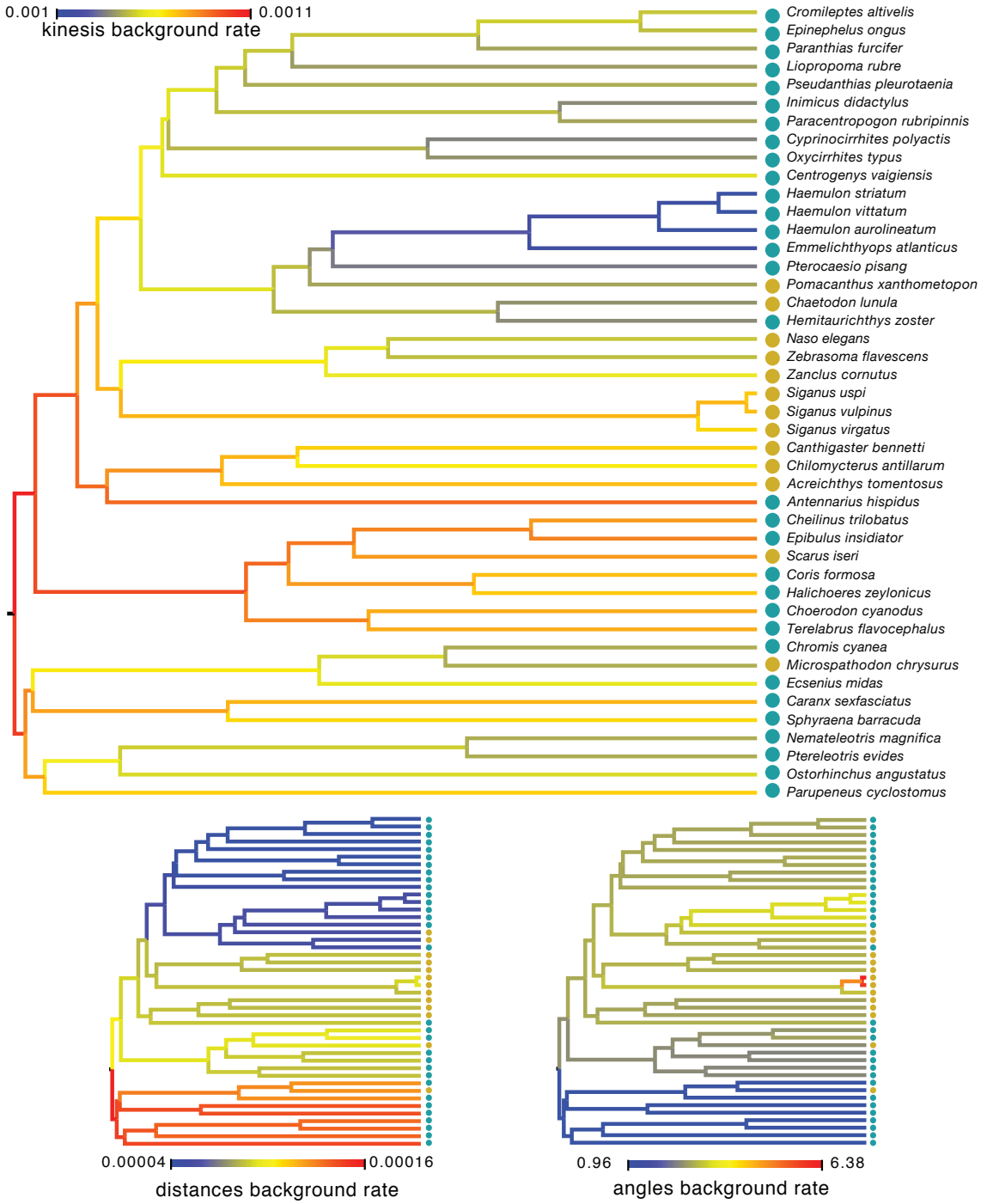

Fig. S4. —Background rate of evolution mapped onto the phylogenetic tree for each kinematic trait dataset from Bayesian relaxed clock, state-dependent, multivariate models of evolution. Rates of evolution shown are rate variation that could not be attributed to the discrete trait.

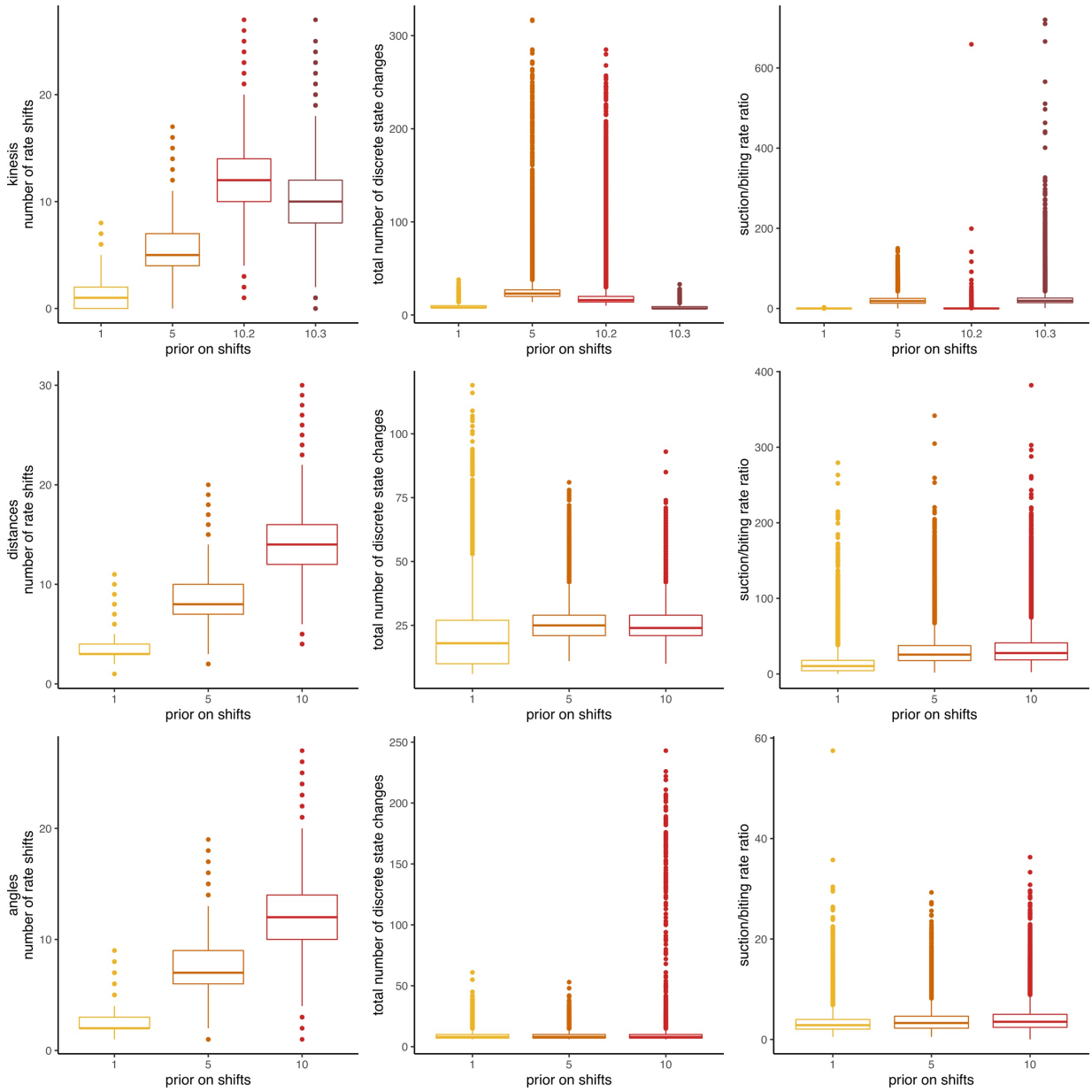

Fig. S5. —Effects of the prior on the number of rate shifts on parameter estimates for Bayesian relaxed-clock, multivariate, state-dependent models of evolution. We find generally consistent parameter results at each value of the prior on the number of rate shifts for distances and angles, but varied effects of the prior on models of overall cranial kinesis. In models of kinesis, "10.2" is a 10-shift-prior model run for 2 million generations of the MCMC, and "10.3" is a 10-shift-prior model run for 3 million generations.

110 SUPPLEMENTAL TABLES

111 *Table S1*.—List of species used in this study with feeding mode designation.

Species	Family	Feeding mode
Acreichthys tomentosus	Monacanthidae	biting
Antennarius hispidus	Antennariidae	suction feeding
Canthigaster bennetti	Tetraodontidae	biting
Caranx sexfasciatus	Carangidae	suction feeding
Centrogenys vaigiensis	Centrogenidae	suction feeding
Chaetodon lunula	Chaetodontidae	biting
Cheilinus trilobatus	Labridae	suction feeding
Chilomycterus antillarum	Diodontidae	biting
Choerodon cyanodus	Labridae	suction feeding
Chromis cyanea	Pomacentridae	suction feeding
Coris formosa	Labridae	suction feeding
Cromileptes altivelis	Serranidae	suction feeding
Cyprinocirrhites polyactis	Cirrhitidae	suction feeding
Emmelichthyops atlanticus	Haemulidae	suction feeding
Epibulus insidiator	Labridae	suction feeding
Epinephelus ongus	Serranidae	suction feeding
Escenius midas	Blenniidae	suction feeding
Haemulon aurolineatum	Haemulidae	suction feeding
Haemulon striatum	Haemulidae	suction feeding
Haemulon vittatum	Haemulidae	suction feeding
Halichoeres zeylonicus	Labridae	suction feeding
Hemitaurichthys zoster	Chaetodontidae	suction feeding
Inimicus didactylus	Synanceiidae	suction feeding
Liopropoma rubre	Serranidae	suction feeding
Microspathodon chrysurus	Pomacentridae	biting
Naso elegans	Acanthuridae	biting
Nemateleotris magnifica	Microdesmidae	suction feeding
Ostorhinchus angustatus	Apogonidae	suction feeding
Oxycirrhites typus	Cirrhitidae	suction feeding
Paracentropogon rubripinnis	Tetrarogidae	suction feeding
Paranthias furcifer	Serranidae	suction feeding
Parupeneus cyclostomus	Mullidae	suction feeding
Pomacanthus xanthometopon	Pomacanthidae	biting
Pseudanthias pleurotaenia	Anthiinae	suction feeding
Ptereleotris evides	Microdesmidae	suction feeding

Pterocaesio pisang	Lutjanidae	suction feeding
Scarus iseri	Scaridae	biting
Siganus uspi	Siganidae	biting
Siganus virgatus	Siganidae	biting
Siganus vulpinus	Siganidae	biting
Sphyraena barracuda	Sphyraenidae	suction feeding
Terelabrus flavocephalus	Labridae	suction feeding
Zanclus cornutus	Zanclidae	biting
Zebrasoma flavescens	Acanthuridae	biting

112

113 *Table S2.*—Morphological disparity analyses.

Trait	Biters Variance	Suction Variance	Variance ratio	p-value
kinesis	0.0016	0.018	10.93	0.02
upper jaw protrusion	1.85e-04	2.01e-03	10.87	0.11
maximum gape	9.37e-04	3.06e-03	3.27	0.04
upper jaw rotation	39.85	379.03	9.51	0.01
lower jaw rotation	104.29	348.21	3.34	0.02
head rotation	4.71	107.92	22.91	0.00
buccal depression	1.68e-05	5.68e-04	33.89	0.01

114

115 *Table S3.*—Results from phylogenetic ANOVAs.

Regression	d.f.	p-value	F-value
overall cranial kinesis ~ feeding mode	1,42	$p < 0.01$	8.63
upper jaw protrusion ~ feeding mode	1,42	$p < 0.05$	4.97
upper jaw rotation ~ feeding mode	1,42	$p < 0.01$	7.46
buccal depression ~ feeding mode	1,42	$p < 0.05$	6.62
head rotation ~ feeding mode	1,42	$p < 0.01$	8.81
lower jaw rotation ~ feeding mode	1,42	$p = 0.15$	2.09
maximum gape ~ feeding mode	1,42	$p < 0.05$	4.72

116

117

Table S4.—Loadings from a principal component analysis.

component	PC1	PC2	PC3	PC4	PC5	PC6
upper jaw protrusion	0.30	0.66	0.37	-0.11	0.15	-0.42
maximum gape	0.37	-0.46	-0.26	-0.10	0.68	-0.19
upper jaw rotation	0.35	0.47	-0.42	0.45	0.24	0.43
lower jaw rotation	0.39	0.08	-0.45	-0.65	-0.43	0.13
buccal depression	0.40	-0.23	-0.14	0.55	-0.50	-0.47
head rotation	0.40	-0.24	0.53	0.10	-0.14	0.59
cumulative variance explained	0.66	0.84	0.90	0.95	0.98	1.00

SI REFERENCES

Beaulieu J.M., Jhwueng D.C., Boettiger C., O'Meara B.C. 2012. Modeling stabilizing selection: Expanding the Ornstein-Uhlenbeck model of adaptive evolution. Evolution. 66:2369–2383.

Moore B.R., Höhna S., May M.R., Rannala B., Huelsenbeck J.P. 2016. Critically evaluating the theory and performance of Bayesian analysis of macroevolutionary mixtures. Proc. Natl. Acad. Sci. 113:201518659.

Revell L.J. 2012. phytools: An R package for phylogenetic comparative biology (and other things). Methods Ecol. Evol. 3:217–223.